

PIERS 2011 Marrakesh

Progress In Electromagnetics Research Symposium

Proceedings

March 20–23, 2011
Marrakesh, MOROCCO

www.emacademy.org
www.piers.org

PIERS 2011 Marrakesh Proceedings

Copyright © 2011 The Electromagnetics Academy. All rights reserved.

Published by

The Electromagnetics Academy

777 Concord Avenue, Suite 207

Cambridge, MA 02138

www.emacademy.org

www.piers.org

ISSN: 1559-9450

ISBN: 978-1-934142-16-5

RFID from Farm to Fork: Traceability along the Complete Food Chain

I. Cuiñas¹, L. Catarinucci², and M. Trebar³

¹Dept. Teoría do Sinal e Comunicaci3ns, Universidade de Vigo, Spain

²Dept. of Innovation Engineering, University of Salento, Lecce, Italy

³Faculty of Computer and Information Science, University of Ljubljana, Slovenia

Abstract— The project “RFID from Farm to Fork” looks for the extension of RFID technologies along the complete food chain: from the farms where cows, fishes, sheep, grapes, etc. grow; to the final consumer at the supermarkets, including all intermediate stages: transports, factory processes, storage. The paper is intended to show the project objectives and concerns, as well as it highlights the main radio propagation problems detected within a RFID system installed in a food factory. The paper also shows a proposal of using RFID traceability in different study cases.

1. INTRODUCTION

People need to eat! For this reason, the production and distribution of food is the largest and the most important activity in each country all over the world. Because of this extension of food economy, different new proposals appear to improve the quality of the products and the information received by the consumers.

This paper has the aim to present the works developed along the project “RFID from Farm to Fork”, a CIP-Pilot action involved within the 7th Frame Work of the European Union. Our proposal looks for the extension of RFID technologies [1] along the complete food chain: from the farms where cows, fishes, sheep, grapes, etc. grow; to the final consumer at the supermarkets, including all intermediate stages: transports, factory processes, storage. The main objective is the use of only one system to perform the complete traceability, recording data at each stage. These data could be useful to determine the perfect condition of the final product, but also to control the process during the elaboration. Thus, both final consumers and producers would take advantage of such systems.

The final consumers could obtain different data above the whole process suffered by the product they are buying, just by moving the object (labeled with a RFID tag) in the surroundings of a RFID reader, which can be installed in the supermarket or even as an application at each personal smart phone. The individual identification of the product allows the software to obtain a complete traceability report from a central database, and to bring the consumer this information. Each of the producers along the chain could use the identification by radio frequency to control his production and storage, and to know some previous information of his ingredient matters. The project involved both the design of the complete system and its tests at different stages of the chain: fishing companies, wine producers, food transporters, and final users, in order to define the actual interest of the system, its performance, and its advantages and disadvantages.

The following sections show the proposal of the project, the radio propagation difficulties in factory ambient, as well as an introduction to some of the pilot tests.

2. THE RFID F2F PROPOSAL

The project will showcase the ability of RFID technologies to make a return on investment for SMEs in the food industry, as well to provide large information to the consumers [2]. The opportunities for such a return on investment arise from the following:

- Opportunities to create markets for premium products (organic, etc.) if technology can address authentication, condition monitoring and quality control.
- New opportunities are created to increase quality, reduce wastage, reduce energy used for refrigeration, reduce chemical usage for preservatives, optimize carbon use, etc.
- Impact on competitiveness and productivity gains.
- Potential for new markets for food producers in the regions.
- Increased productivity through reduced wastage.

- Authentication of origin, process and transport of products.

These advantages have been realized in large concerns, which have control over most or all of the value chain and are in a position to make an end-to-end investment. However, they are not available to independent SMEs, which only participate in one stage of the value chain. By linking RFID and sensor network technologies with a Europe wide database, which can store the exact history of any food product, SMEs will be given the opportunity to optimize their own business process to maximize return. In addition, a pan-union resource will be created which will allow producers to demonstrate unequivocally the quality and freshness of their product, which will have the effect both of increasing consumer confidence, and increasing producer margins.

The emphasis of the current project is somehow advanced from previous projects, in that it proposes:

- Integration of RFID and sensor networks to provide end to end monitoring.
- Demonstration of end-to-end traceability for the whole value chain in a number of different product areas.
- Integration with an international database of food ingredients.

3. RADIO WAVE PROPAGATION IN FOOD FACTORY AMBIENTS

The use of RFID and/or sensor networks in the food chain has been previously tested, and it could obviously provide a competitive advantage to the involved companies. However, the radio propagation within a factory presents important differences compared to other more friendly environments: there are lots of metallic elements: machinery, store installations, transports, and even walls and ceiling, which limits the performance of the radio systems. When the factory belongs to the food sector, the situation becomes more and more complicated, as most of the food products present a large content in water, which is not the best friend of the radio waves. Even more, some of the packages are metallic (cans or metallic sheets), which are also limitative for the good performance of a radio system.

3.1. Fish Factories

The fish factories, both for freezing or for canning processing, resulted to be problematic for radio electric propagation due to the presence of large amounts of water and ice within the tags and the readers. The fresh fish is commonly transported inside plastic boxes containing the fish and a lot of ice around. This ice content makes really difficult to establish a radio link if the RFID tag is glued directly to the plastic: a solution consists of separating the tag away from the box (i.e., from the ice) to improve the propagation conditions.

Some tests have been performed using plastic boxes with frozen fish, or just fish with water, or even a simple wet box. When the box is dry, the tag can be read from several meters, but in wet conditions the coverage distance is reduced to several centimeters. Once the fish is frozen and packed, the installation of the tag is again a problem: if it is too close to the ice, the performance of the radio link could be reduced. And it is not easy to install a tag far from the ice inside a freezer!

When the final product is the canned fish, the metallic surfaces of the cans act as isolators for the radio links. The installation of the individual tags in a separate section of the carton package could be enough to solve the situation in a supermarket. But it is almost impossible to manage a store of cans, by means of individual RFID tags. Thus, a separate tagging (individual can vs. lots of cans in larger batches) would be needed to control the storage. This solution could also present some problems depending on the side of the box the tag is glued: if the tags fall in the middle of a package island, perhaps the RFID reader is unable to detect the tag information.

3.2. Wineries

When dealing with wine factories, there are different limitations to the propagation along the process from the vineyards to the bottled wine. The grapes are commonly carried from the vineyards to the winery in plastic boxes of around 20 kg. Again, the water contents could be a difficulty, although less important than in fishery.

Part of the process of manufacturing the wine is performed in steel barrels. The building where these recipients are placed does not present good propagation conditions, as a lot of reflectors and scatters are present in such indoor environment. In this situation, the performance of the physical layer of a RFID system could be affected, as various fading events could appear due to the multipath phenomena.

Once the wine is bottled, the location of the tags on the bottle surface is also problematic: the liquid content becomes a good conductor, and so the transmission capabilities of the tag are reduced. A good selection of the type of tags, as well as its location in the body of the bottle, is a key factor to achieve valid performances.

4. CASE I: WINE PRODUCTION

The quality and the taste of a wine depend on many factors: type of grape, soil, percentage of precipitation and temperature during grapes growing, eventual use of pesticides, types of harvest (day or night), storage conditions of grape before of wine making, and so on.

Experts wine consumers, therefore, are becoming more discerning and pretend to know as much data as possible in order to enlarge their knowledge, be sure of the authenticity of a wine and spend consciously.

One of the several pilots related to the wine supply chain is a small winery named “Vigne Mastrodomenico” located in Basilicata, a Region of Southern Italy, and producing no more than 10000 bottles per year of “Aglanico del Vulture”. The vines grow on a hilly volcanic soil as large as eight ectars with different degrees of sun exposure depending on the vineyard zone. In some cases, hence, it could be necessary a selective forced irrigation. Once the harvest is done, the grapes are processed in a small winery carved into the rock, creating a natural habitat (for instance, a constant temperature of almost 15°C is naturally achieved) for this kind of wine. The presence of the wine and of steel drums, though, complicates the scenario from an EM point of view.

Two aspects have been considered so far. The first one regards the wireless sensor network (WSN) at the vineyard site, useful to collect both meteorological and soil status data to be associated with the single wine bottle and to automatically activate the forced irrigation. The second one, more critical, regards the RFID-related hardware investigation to be used in the winery. As previously stated, in fact, the presence of electromagnetically hostile materials, such as liquids and metals, makes challenging the single bottle traceability in the different steps of the wine supply chain.

For such a purpose, a very complex RFID-based test bed environment has been assembled. The test bed is capable to evaluate the tag performance in realistic situations and in each step of the wine supply chain. Results in terms of successful read rate as well as of RSSI (Received Strength Signal Indication) have been obtained. These results demonstrate that, among the possible RFID frequency bands, UHF has to be preferred to HF for several reasons. For instance, HF tags do not work properly in Far Field conditions, thus implying the impossibility to be used in some critical steps of the supply chain requiring a far field interrogation. Moreover, they are not EPCGlobal compliant, with relevant consequences in terms of multiple readings, generality of the implemented solution and many others. Consequently, two different UHF readers, three different reader antennas, two different Near Field UHF tags and six different Far Field UHF tags have been tested. With each tag attached to a wine bottle, the reading range has been firstly measured both with and without wine inside, so to characterize each tag on the bases of its tolerance to the liquid presence. Then, the problem of the tag performance degradation when the traceability system is implemented at items level in case of presence of liquid has been investigated. Results in terms of successful read rate have been obtained by varying the mutual orientation between tag antenna and reader antenna (i.e., 0° and ±90°). In Figure 1, for instance, the successful read rate of two near field tags (Cube 2 and Paper Clip) and of a far field one (Jumping Jack) are reported. It is quite evident that in critical conditions far field tags perform better than near field ones. Nevertheless, when different supply chain steps based on longer interrogation distances are considered, the effect of the performance degradation is more marked. The individuation of the best tag positioning on the wine bottle is the next step.

5. CASE II: FISH MANUFACTURING

A fish pilot in Slovenia deals with traceability of seabass grown in northern part of Adriatic sea. At farm, a young fish brought from hatchery is breeding for four years in cages under similar conditions as other fish. On the day of catch, fish is transferred to the processing factory, sorted by weight category and packed into styrofoam boxes depending on orders. In some cases fish is also cleaned or filleted. After that, boxes are covered with ice and transported to cold store. The next day, fish is delivered to retailers, restaurants, fish market and even private consumers.

In the supply chain is very important to secure required temperatures of fish between 0°C and 4°C. This can be easily done by using active RFID data logging device with temperature sensor.

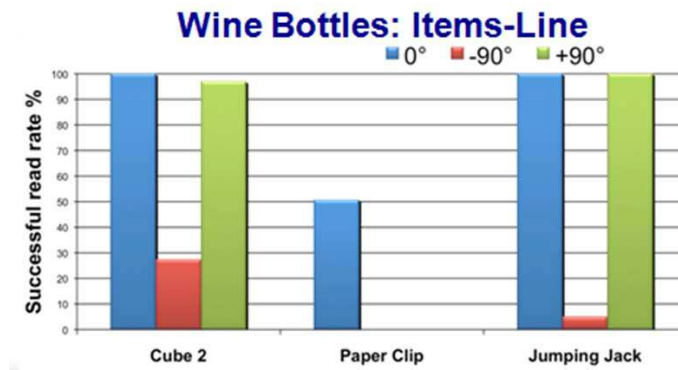


Figure 1: Successful read rate of three commercial tags in the wine items line.

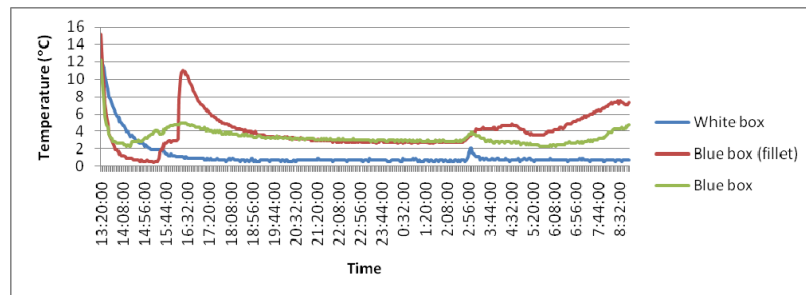


Figure 2: Temperatures measured inside three boxes of fish.

To perform tests in real environment we used two RFID development kits [3], one with IDS-SL900A chip working in UHF frequency bands and the other one with IDS-SL13A in HF frequency bands. Temperatures are automatically measured and recorded, and can be used in a system to automatically notify users about an event.

For the pilot implementation, RFID data loggers will be used to measure the temperature of fish which means that they are placed in the middle of box under the ice before they leave a processing room. By this kind of a solution we start measuring temperatures when fish is packed and read temperatures only at the delivery place. To show a temperature graph during complete supply chain a mobile RFID reader will be used when RFID data loggers are removed from the box.

An example of measured temperatures can give the consumer a clear picture what happened with fish he ordered. Figure 2 shows a temperature graph of three different packages of fish: a) White box — temperatures inside a box where fish was covered by ice; b) Blue box (Fillet) — the process of filleting took place after the sorting process and fish was stored to the blue box and covered by ice packing sheets; c) Blue box — fish was stored to blue box and covered by ice packing sheets. At the end, by the delivery only temperatures of fish covered with ice was more or less the same while in blue boxes temperature starts to increase due to the transport environmental conditions.

6. CONCLUSIONS

This paper presents the objectives and initial work of the project “RFID from Farm to Fork”, highlighting the radio propagation concerns of a RFID system within an industrial environment. Some advances on the application to winery and fish manufacturing processes have been also commented.

Taking into account the electromagnetically complex propagation scenario of a winery and of a wine supply chain, an exhaustive tag characterization has been carried out and the performance degradation due to the presence of liquid has been confirmed. Once proved that, in the wine production case, UHF tags must be preferred to HF ones. The performance comparison of both near field and far field UHF tags in a practical scenario has been performed and the better suitability of far field tags has been pointed out.

Vice versa, as for the fish manufacturing case, RFID data loggers were used to measure and store

temperatures inside a box of fish covered with ice. This data can be used to control the conditions of perishable food in the supply chain. The proposed implementation is based on radiofrequency identification and does not require the use of any additional sensor networks communication technology. The results were very similar for both systems (HF and UHF) used in the described scenario.

ACKNOWLEDGMENT

This work has been supported by European Union (CIP-Pilot Actions), under the project “RFID from Farm to Fork”, grant agreement number 250444.

REFERENCES

1. *RFID Journal*, <http://www.rfidjournal.com>.
2. RFID-F2F From Farm to Fork, <http://www.rfid-f2f.eu/>.
3. IDS-SL13A Smart Label Chip with Sensor & SL 900A, EPC Class 3 Chip with Sensor, <http://www.ids.si/>.

Contents

Complex Self-organized Multi-pulse Dynamics in a Fiber Laser: The Rain of Solitons	12
Principal Component Analysis for Low-dimensional Modeling of Mode-locked Lasers	17
Extraordinary Transmission and Light Confinement in Subwavelength Metallic Films Apertures	22
Transmission Properties of Dual-period Arrays of Cylinders	27
Scattering Properties of Elliptical Cylinder Coated by Lossy DNG Metamaterial	32
Enhanced Ferromagnetic and Ferroelectric Properties of La Doped Multiferroic $\text{Bi}_5\text{Fe}_{0.5}\text{Co}_{0.5}\text{Ti}_3\text{O}_{15}$ Ceramics	37
Enhanced Absorption in Si Solar Cells via Adding Thin Surface Plasmonic Layers and Surface Microstructures	41
Layer-structured $\text{Bi}_5\text{F}_{0.5}\text{Co}_{0.5}\text{Ti}_3\text{O}_{15}$ Thin Films Grown by Pulsed Laser Deposition	45
Light Trapping within the Grooves of Diffraction Gratings	49
Nondestructive Evaluation of Extended Scatterers Using Phaseless Data Subspace-based Optimization Method in the Framework of the Method of Moments	56
Theoretical Model for Optical Sensing of a Random Monolayer of Particles	61
CAROLS SMOS CAL/VAL Campaigns	65
Radio Frequency Interferences Investigation Using the Airborne L-band Full Polarimetric Radiometer CAROLS	70
Interpretation of CAROLS L-band Measurements in the Gulf of Biscay (September 2007)	75
Retrievals of Soil Moisture and Optical Depth from CAROLS	80
A Compact Single Feed, Low Cost Broadband Switched-beam Antenna for Mobile Wimax Applications	85
Compact MIMO Microstrip Antenna with Defected Ground for Mutual Coupling Suppression	89
Performance and Capacity Analysis of Compact MIMO Aided OFDM-SDMA Systems	93
Wide-Band Rectangular Dielectric Resonator Antenna for Wireless Applications	98
A Very Small UWB Dielectric Resonator Antenna for Mobile and Wireless Communications Systems	102
A Super-miniaturized Low Profile Antenna on a Substrate of Rose Curve Resonators	106
Thermographic Analysis of Swiss Albino Mice Exposed to 1.8 GHz GSM Frequency	110
Influence of a Dielectric Insert of High Permittivity on the Transmit Performance of a 300 MHz Multi-channel MRI Loop Array	116
Electromagnetic Compatibility between Implantable Cardiac Pacemakers and RFID Systems: Experimental Set-up, Test Protocol and Preliminary Results	121
Impedance Variation of an Equipment under Test in a GTEM Cell	125
Design Optimisation to Reduce the Magnetic Fields Propagated from DC Light Rail Transit Systems	131
Experimental Dynamical Evolution of Impulse and Delta Pulses through Dispersive Vegetation in Remote Sensing Frequency Bands	137
Investigation on a Ladder-shaped Frequency Selective Surface for Dual-band Operation	141
Maxwell's Motor Equation and the Mechanical Power	144

Analysis of Light-beam Scattering from DWDD Disk with Control Layer under Considering Rear Process	149
Electromagnetic Wave Propagating in Gyroelectric Slab in the Perpendicular Configuration	152
Three Dimensional FDTD Analysis of Near-field Optical Disk	157
Mapping Technique of Basic Magnetic Field in MR Tomography	161
Modelling of 3D Thin Regions in Magnetostatic NDT Using Overlapping Elements in Dual Formulations	166
Design and Study of a Permanent Magnet Synchronous Motor for an Electric Compressor	171
Full-wave Mode Analysis of Asymmetric Coupled Microstrip Structures: Particular Case of Quasi-symmetric Lines	176
2D PIM Simulation Based on COMSOL	181
A Novel Approach for Modeling Diodes into FDTD Method	186
Magnetic Susceptibility Modelling Using ANSYS	190
Simulation of Defects in Photonic Band Gap Structures	194
Microstrip Ultra-Wide-Band Filter	198
Study on Electromagnetic Properties of Reinforced Concrete Construction Wall	201
Effect of Friction Layer Creep Deformation on Dynamic Behavior of Traveling Wave Rotary Ultrasonic Motor	205
Doorway State Mechanism with Electromagnetic Waves in the Optical Regime	209
A Hemi-directional Antenna Array Concept for Automotive Radar	213
A Dual Polarization Bow-tie Slot Antenna for Broadband Communications	217
Broadband Fractal Circular-monopole Antenna	222
A Monopole Antenna with CPW-fed for Digital Video Broadcasting Applications	228
Reflection Characteristics of Microstrip Base on Finite Element Method	231
Circularly Polarized Rectangular Microstrip Antenna Using Ring Slots on the Ground Plane	235
Resonance of Rectangular Microstrip Patch over Ground Plane with Rectangular Aperture in the Presence of High-permittivity Dielectric Layer below the Aperture	239
Detailed Modified Iwasawa Decomposition of Ray Transformation Matrix and Its Applications	242
Radon-Wigner Display Implemented by Spatial Light Modulators	246
Orbital Angular Moment Density of Beam Given as a Superposition of Hermite-Laguerre-Gauss Functions	250
Light Propagation in Tapered Optical Fibers: Spatial Light Confinement and Generation of Plasmonic Waves	255
First-order Optical Systems: Radon-Wigner Transform Approach	259
Wigner Based Analysis of Geometric Related Resolution Degradation and Geometric Super Resolution Configurations	262
Partially Coherent Ambiguity Functions for Depth-variant Point Spread Function Design	267
Complex Amplitude Filters for Extended Depth of Field	273
Temporal Similarity for Short Pulses	276
Conditions for Photon-particle Interactions	280
Investigation of Ionospheric Slab Thickness Behaviour over Cyprus during Minimum Solar Activity ...	286
A Study of Es Layer Characteristics over Cyprus	290
Integral Localized Approximation Description of v -th Order Bessel Beams in the Generalized Lorenz-Mie Theory and Applications to Optical Trapping	294
Genetic Algorithms Application for the Optimal Design of Magnetic Vagus Nerve Stimulator	299

Asymmetrical Stripline Based Method for the Electromagnetic Characterization of Metamaterials	305
Design and Fabrication of Random Optical Surfaces by a Modified Speckle-based Method	310
A New Multi-ring SRR Type Metamaterial Design with Multiple Magnetic Resonances	315
Active Earth Observation from Unmanned Aerial System	320
Undersampled Digitally Heterodyned SFGPR with Variable Sampling Frequency	325
Using of Multi-angular Radiometric Measurements for Short Wind Wave Parameters Estimate	329
Development of Circularly Polarized Synthetic Aperture Radar (CP-SAR) Onboard Small Satellite	334
System Aspects of Mutual Coupling in Reconfigurable Active Phased Array	342
An Interpretation of Maxwell Equation by Using the Formalism of Gravitational Waves	348
Velocity Curl and Spin in Electromagnetic Fields	352
Theorem for the Identity of the $L(c, n)$ and $\hat{L}(\hat{c}, \hat{n})$ Numbers and Its Application in the Theory of Waveguides	357
Electromagnetic Sources and Observers in Motion VI — New Motional Optics	362
Electromagnetic Sources and Observers in Motion V — A Revised Theory of Relativity	367
Efficient Use of “White Spaces” in the UHF Band (470–862 MHz) Employing Genetic Algorithms	373
A Planar Parabolic Patch Antenna for UWB Applications	377
A Novel Compact Ultra-wideband Rectangular Shaped Antenna	381
A Novel Printed Circular Antenna for Ultra Wideband Applications	386
Circular Patch Antenna Directivity Enhanced by Left-handed Material Cavity	390
Coupled Non Uniform Transmission Lines: Modeling and Crosstalk Performances	395
Design of Non Uniform Meander Line Antennas for Passive RFID Tags in the UHF Band	400
Design of Composite Electromagnetic Wave Absorber Made of Fine Spherical Metal Particles Dispersed in Polystyrene Resin	404
Identifying EMC Interference Sources of a Microwave Transmission Module in Order to Locate Them	411
Low Frequency Monopole-like Small Metamaterial Antenna	415
Optimization of a Patch Antenna Performances Using a Left Handed Metamaterial	419
Global Maps of TEC and Conditions of Radio Wave Propagation in the Mediterranean Area	422
Analysing the Attenuation at Mobile Phone Bands Provided by Vegetation Supported by Lattice Structures	427
Microstrip Antenna for Microwave Imaging Application	431
Propagation Characteristics of 24 GHz Frequency Band for Automotive Collision Avoidance Radar	435
Swept Versus Real-time Spectrum Analyzer Ability to Accurately Asses Electromagnetic Exposure due to Wireless Communications Signals in the Environment: An Analysis	438
Frequency Tuned Planar Inverted F Antenna with L Shaped Slit Design for Wide Frequency Range	443
Beam Steering of Time Modulated Antenna Arrays Using Particle Swarm Optimization	448
The Compact Design of Dual-band and Wideband Planar Inverted F-L-antennas for WLAN and UWB Applications	453
The Application in Spacecraft of High Temperature Superconducting Magnetic Energy Storage	458
Comparison Study of Eddy Current Losses of Induction Motors Fed by SPWM and SVPWM Inverters	461
Regulatory Analysis of the Intermodulation Interference between the PCS Receiver and the Low-power Radio Devices	466
Statistical Characteristics of Region Propagation of Decametric Radiowaves in Time of Heliogeophysical Disturbances	471
Soil Parameters Retrieval Using a Neural Network Algorithm Trained by a Two Layers Multi-scale Bi-dimensional SPM Model	476

Accuracy of Wind Field Deduced from Envisat WSM SAR Images along the Range	480
Combined Direct and Remote Sensing Measurements of Wave Parameters at the off-shore Research Platform in the Black Sea	483
RCS Simulations on Wet Corner Reflectors with SBR Code SIGRAY	488
Development of THz Coherent Sources Using Quantum Cascade Lasers	491
Modeling by FDTD of Some Optical Properties of Photonic Crystals Based on a Nanocomposite of Silver in TiO ₂	495
Materials Adsorption Characterization by Random Coherent Electromagnetic Waves	499
A Proposal for a Low-cost TO-can 25-Gb/s Laser Diode Package	502
1D Inversion of Multi-component and Multi-frequency Low-induction Number EM Device (PROMIS) for Near-surface Exploration	507
3D Laser Imaging	512
Amplified Stimulated Terahertz Emission from Optically Pumped Graphene	517
Recent R&D Trends in Broadband Optical Access System Technologies towards the Second-generation FTTH Era in Japan	520
A New Configuration of Broadband Wireless Access in Heterogeneous Ubiquitous Antenna and Its Experimental Investigation	524
Radio Agents Technologies for Wireless-as-a-service Network	529
Next Generation Free Space Optics System for Ubiquitous Communications	534
Checking of Combustion Chamber of Rocket Using ECT with AMR Sensor	540
Estimation of Reinforcing Bars by Using Real GA with Discrete Chromosomes	543
A Comparison of Focusing Algorithms for Ground Based SAR System	548
Imaging of Wide-angle Near-field Inverse Synthetic Aperture Radar Data Using Back-projection Algorithm	554
Novel Symmetrical EH-horn Antennas Based on EBG Technology	558
Developments Low Cost Probe Compensated Cylindrical Near Field Measurement for Antenna Radiation Wave	561
A Circularly Polarized Microstrip Antenna Array with a Binomial Power Distribution	565
Performance Characteristics of a Dual-sense Helical-beam Antenna	569
Analytical Prediction of Feed Efficiency in Offset Gregorian Reflector Antennas with Non Planar Log-periodic Type Feeds	573
Study of Microstrip Patch Resonator Printed on Anisotropic Substrate Characterized by Permittivity and Permeability Tensors	578
Design of Flat Gain UWB Tapered Slot Antenna for on-body Concealed Weapons Detections	581
Surface Wave Enhancement Using HF Metamaterials	586
Consequences of Localization of Non-linear Effects in Magnetic Dots	589
Evidence of Ducting Mode Electromagnetic Wave Propagation in the Indoor Environment	593
Some Examples of Uncorrelated Antenna Radiation Patterns for MIMO Applications	598
Clustering Impact on the Statistics of the Multipole Expansion Coefficients of a Wireless Channel	603
Space Diversity Evaluation in Millimeter Band Wireless Communication Systems	608
Angle of Arrival and Doppler Spectrum in the Presence of Generalized Two-dimensional Anisotropic Scattering	613
A New Approach for Measurements of Signal Level Contents in a Real Wireless System in the City of Curitiba, Brazil	618
Design of Lightning Systems with Usage Sensitivity Analysis for Improvement of Numerical Model	623
Artifact Removal Algorithms for Microwave Imaging of the Breast	627

Influence of Weak Electromagnetic Fields on Cerebrovascular System of the Person	630
Interpolation of 3D Magnetic Resonance Data	635
Homogeneous Phantom Model vs. Visible Human Dataset: Impact on MRI-induced Heating of Metal Implants	639
Design and Fabrication of Planar Magnetoinductive Resonator Arrays for MRI System Field Shaping ..	643
Measurement of Concentration and Mobility Spectrum of Air Ions in the Natural Environment	648
Cryogenic Technique for Cancer Destroying Optimalization	653
Image Reconstruction by EIT with Usage NMR	657
Utilization of Boundary Conditions in MR Image Reconstruction	661
The Vagarious Dispersive Behavior in a Magnetically Uniaxial Metamaterial around the Plasma Frequency	665
A Novel Preconditioner Based on CSL Operator for Solving the Helmholtz Equations	669
The Characteristics of 116 Ore Belt in the Shihu Gold Deposit of Western Hebei — Based on the EH-4, China	672
Application of EH4 in the II Forecast Area of Yushiwa Iron Mine of Hanxing Area, China	676
Validity of Image Theorems under Spherical Geometry	680
A Novel and Simple Analytical Method for Analysis of AMC and EBG Properties of Lossless Artificial Impedance Surfaces	685
Full Wave Analysis of Finite Uniform Metallic Grid FSS under Oblique Incidence Using Scale Changing Technique	689
Rapid Idea of Located Defects on Grounding Systems	693
Model to Predict Losses in the Permanent Magnets for Dynamic Applications	699
Analytical Model of TeraHertz Frequency Voltage Noise in Schottky-barrier Diodes and Heterostructure Barrier Varactors	702
Application of EH4 in the Zhayaoku Area of Fushan Iron Mine of Hebei, China	706
Terahertz Current and Voltage Noise in Nanometric Schottky-barrier Diodes	710
A Set of New SDA Basis Functions with Strongly Decaying Properties	714
Novel FDTD Method with Low Numerical Dispersion and Anisotropy	718
The Equivalent Rest-mass of Photon	723
A Mechanical Effect Induced by Electromagnetic Radiation May Explain the Wave Function Collapse of a Quantum Object	726
Quantum Mechanics Suggests that Photons with Different Energy Do Not Travel at the Same Speed ..	729
Low Frequency Surface Plasmon Polaritons on a Periodically Structured Metal Strip with High Confinement of Fields	734
Selective and Collaborative Optimization Methods for Plasmonics: A Comparison	737
Electromagnetic Heat-induced in Meso-structures: Computation of Temperature in Metallic Dimers ..	742
Generation of Encryption Keys from Plasmonics	747
Design and Fabrication of a Modular Eddy Current Micro Sensor	752
Wireless Electronic Structural Surveillance Sensors Using Inductively Coupled Sacrificial Transducers ..	756
A Meta Model for Damage Prognosis of Concrete Structure	761
Multi Agent System for Agile Wireless Sensor Network to Monitor Structures	765
Optical Image Analysis Based Concrete Damage Detection	771
Sensors-based Noise Removal Method from Pile Integrity Test (PIT) for Concrete Marine Piles	775
Sub-surface Concrete Structure Damage Quantification Using TIR and Visual Inspection	781

Infrared Thermography for Assessing and Monitoring Electrical Components within Concrete Structures	786
Detection and Quantification of Corrosion Damage Using Ground Penetrating Radar (GPR)	790
Radar-based Quantification of Corrosion Damage in Concrete Structures	794
Determining the Effect of Faraday-rotation and Optimum Rotation Angle in Different Types of Magneto-optical PBG Structures	799
Underwater Communication Systems: A Review	803
Novel Techniques for UWB Microwave Imaging of Objects with Canonical Shape	808
High Resolution Optical Profilometry Using Diffractive Tomographic Microscopy	813
Experimental Study on Imaging Algorithm with Simple UWB Radar for a Target with Translation and Rotation	818
Miniaturized Printed Yagi Antenna for 2.45 GHz RFID Readers	822
A Matrix-vector-potential Analysis of the Bi-elliptical Toroidal Helical Antenna	825
Design of an Antenna with Reconfigurable Band Rejection for UWB Cognitive Radio	830
Overview of Reconfigurable and Compact Antennas Using a Magneto-dielectric Material	834
A Frequency Reconfigurable Microstrip Rectangular Patch Antenna Using Stubs	839
Modeling and Simulation of Temperature Distribution in Laser-tissue Interaction	844
Using Bioheat Equation 3D WEB-spline Prediction of Ocular Surface Temperature	848
On the Integration of Behavioral Component Descriptions in the Full-wave Transmission-line Modeling Method	853
3D FEA of SMPM Accounting for Skew and End Windings	858
Performance Improvement of Different Topologies of Claw Pole TFPM Based on a 3D FEA	861
On the Iron Losses Computation of a Three Phase PWM Inverter-fed SMPM by Using VPM and Transient FEA	866
The Methods of Measuring Attenuation of Thin Absorbent Materials Used for Electromagnetic Shielding	870
Small Chambers Shielding Efficiency Measurements	875
Procedure for Absorption Measurements of Absorbing Materials	880
Multilayer Microstrip Antenna on Flat Base in the X Band (8.5 GHz–12 GHz)	885
Active Microstrip Antennas Operating in X Band	890
Efficient Method of 3G Signal Detection	895
MIMO Implementation with Alamouti Coding Using USRP2	899
Optoelectronic Phase Noise System Designed for X-band Sources Measurements in Metrology Applications	903
Application of EH4 in the I Forecast Area in Yushiwa Iron Deposit of Hanxing Area, China	907
Determination of Thermal Model Parameters for Stator Slot Using Numerical Methods	911
The Physical Regularization of Incorrect Electrodynamical Problems	915
Novel Concept of ENG Metamaterial in Rectangular Microstrip Patch Antenna (Partially Loaded Case) for Dual Band Application	920
Input Impedance Calculation for Coax-fed Rectangular Microstrip Antenna with and without Airgaps Using Various Algorithms	924
Helically Corrugated Feed Antenna with Far out Sidelobes Reduction	928
Design and Development of Monopulse Dual Mode Corrugated Horn	931
Novel Application of MNG Metamaterial in Rectangular Microstrip Patch Antenna (Partially Loaded Case) for Dual Band Application	935

Novel Design of Dual Band Rectangular Microstrip Patch Antenna Partially Loaded with MNG Meta-material for S-band Application	939
New Formulation of the Method F.W.C.I.P. for the Modelling of a Planar Circuit Integrating a via-hole	943
Fine Synchronization with UWB TH-PAM Signals in Ad-Hoc Multi-user Environments	948
Performance Parameter of Hybrid Wireless-optical Broadband-access Network (WOBAN): A Study on the Physical Layer of Optical Backhaul and Wireless Front-end	953
Properties of Spread-F in High and Low Latitude Ionospheres	958
Monitoring of Thermal Dome as an Iridescent Sphere above the Atmosphere	962
Monitoring of Thermal Dome in the Earth Surface Layer	964
Monitoring of Thermal Dome Shock Front Pattern on the Earth	968
Author Index	972

Contents

Circuit Simulation of Varactor Loaded Line Phase Shifter	987
Development of a Double-clad Fiber Laser Simulator for the Design of Laser Cavities with Specific Applications	991
Maize Crop Yield Map Production and Update Using Remote Sensing	995
Adaptive RF Power Amplifier Tuned with Ferroelectric BST Varactor	999
Practical Use of the Kramers-Kronig Relation at Microwave Frequencies. Application to Photonic Like Lines and Left Handed Materials	1003
Coaxial Quasi-elliptic Filter Using a Suspended Resonator and Vertically Stacked Coaxial Lines	1010
Asymmetric Microstrip Right/Left-handed Line Coupler with Variable Coupling Ratio	1013
A Dual-band Wilkinson Power Divider Utilizing EBG Structure	1018
Large Scale Measurement of Microwave Electric Field Using Infrared Thermography and Electromagnetic Simulation	1021
Numerical Study of a Coplanar Zeroth-order Resonator on YIG Thin Film	1025
Metallic Absorptivity at Normal Incidence above Far-infrared	1029
Enhanced SBS Instability Growth Rate of Extraordinary Electromagnetic Waves in Strongly Coupled, Magnetized Plasma	1033
On the Electrokinematics of Counter Propagating Transverse-electric and Transverse-magnetic Waves in the Absorbing Plate in a Waveguide	1038
Harmonic Imaging through Nonlinear Metamaterial Surfaces	1043
Generation of Waves by a Neutron Beam in a Quantum Plasma of Nonzero Spin. An Influence of the Spin-orbit Interaction	1047
Horn Antennas Loaded with Metamaterial for UWB Applications	1052
Use of the Neural Net for Road Extraction from Satellite Images, Application in the City of Laghouat (Algeria)	1057
Novel Compact RFID Chipless Tag	1062
RFID Tag Antenna Design on Metallic Surface by Using Rectangular Micro-strip Feed	1067
Simplified Design Approach of Rectangular Spiral Antenna for UHF RFID Tag	1071
Experimental Verification of Snell's Law at Sub-optical Frequencies	1080
Backward Wave Modes of Partially Plasma Column Loaded Cylindrical Waveguide	1084
Scattering Analysis of a Submerged Conducting Object in Lossy Media via Low Frequency EM	1089
The Feature Selective Validation (FSV) as a Means of Formal Validation of Electromagnetic Data	1094
Comparing EMC-signatures by FSV as a Quality Assessment Tool	1099
On the Psychological Processes of Decision Making in Displays of Electromagnetic Data	1104
Numerical Noise Reduction in the Fourier Transform Component of Feature Selective Validation	1109
Study of Transient Phenomena with Feature Selective Validation Method	1113
Performance Improvement of FSV in a Special Situation	1118

Supplement on the Non-constancy of Speed of Light in Vacuum for Different Galilean Reference Systems	1123
Permittivity of Vacuum and Speed of Light in Vacuum which Vary with Relative Speeds of Media in Uniform Rectilinear Motion with Respect to Each Other	1127
Reconstruction of Tumors in Human Livers by Magnetic Resonance Imaging	1131
C-ring Metamaterial in Close Field	1134
Sensors and Experimental Model Development for PD Localization in HV Transformers	1139
Comparison of Different Methods for Measurement of Shielding Fabrics Properties	1144
Propagation of Electromagnetic Wave in Layered Heterogeneous Medium	1149
Measurement of Concentration and Water Flow	1153
Using Metamaterials as Electromagnetic Lens for MR Tomograph	1158
The Design of High-impedance and High-voltage Input Amplifier for Measurement of Electropotentials on Solid-liquid Phase Boundary	1162
Analytical Expressions of Diffraction' Free Beams Obtained by Diffraction on an Opaque Disk	1167
Rescaled Range Analysis of ELF Natural Electromagnetic Noise from Antarctica	1171
Hybrid Method to Compute the Magnetic Field in Bird Cage Coil for a Magnetic Resonance Imaging System	1175
Coils and Magnets: 3D Analytical Models	1178
Discussion on the Magnetic Pole Volume Density in Analytical Models of Permanent Magnets	1185
A Peak to Average Power Ratio Reduction of Multicarrier CDMA System Using Error Control Selective Mapping	1193
Detection of Singularities by Wavelet Technique for Extracting Leaky Waves in Piezoelectric Material	1197
Electromagnetic Study of Planar Periodic Structures Using a Multi-scale Approach	1202
Study of Edge Effect of 4340 Steel Specimen Heated by Induction Process Using Axi-symmetric Simulation	1207
Optimization of Hardness Profile of Bearing Seating Heated by Induction Process Using Axisymmetric Simulation	1214
A Time Domain Hybrid Approach to Study Buildings Connected by Cables	1219
The Effect of Metamaterial Patterning to Improve the Septum GTEM Chamber Performance	1224
The Integration of the Multihoming Concept in Ad Hoc MANET Mobile Networks	1229
Electromagnetic Compatibility of CMOS Circuits along the Lifetime	1235
Reconfigurable RF-MEMS Metamaterials Filters	1239
Optimization of Coherence Multiplexed Coding for High Density Signal Processing	1243
Highly Birefringent Photonic Crystal Fiber for Coherent Infrared Supercontinuum Generation	1247
On the Role of Maxwell Fields in the Resonant Transfer of Energy	1252
Raman Response of a Highly Nonlinear As ₂ Se ₃ -based Chalcogenide Photonic Crystal Fiber	1256
Generation and Detection of Terahertz Radiation by Field Effect Transistors	1261
Terahertz Emission, Detection and Modulation Using Two-dimensional Plasmons in High-electron-mobility Transistors Featured by a Dual-grating-gate Structure	1266
Spin Related Effect in Terahertz Photovoltaic Response of Si-MOSFETs	1272
Design of 2 x 2 U-shape MIMO slot antennas with EBG material for mobile handset applications	1275
Silhouette Coverage Analysis for Multi-modal Video Surveillance	1279
Structural Entropy Based Localization Study of Wavelet Transformed AFM Images for Detecting Background Patterns	1284

A New Spatio-temporal ICA for Multi-temporal Endmembers Extraction and Change Trajectory Analysis	1289
Available Seat Counting in Public Rail Transport	1294
Image Processing Methods for Evaluating Infrared Thermographic Image of Electrical Equipments ...	1299
Fair-weather Atmospheric Electric Field Measurements at the Gaisberg Mountain in Austria	1303
An Engineering Approach in Modeling Lightning Effects on Megawatt-class Onshore Wind Turbines Using EMTP and Models	1308
Consideration on Artificial Neural Network Architecture in Application for Microwave Filter Tuning ..	1313
Area of Phase Shifter Operation of the Azimuthally Magnetized Coaxial Ferrite Waveguide	1318
A Dual Linear Polarization Feed Antenna System for Satellite Communications	1324
Study of a Coplanar Circulator Based on a Barium Hexaferrite Nanocomposite	1329
A Linear Ultrasonic Motor Using a Quadrate Plate Transducer	1334
A Novel LLC Resonant Network for Ultrasonic Motor	1338
Theory and Experiment of the Valveless Piezoelectric Pump with Rotatable Unsymmetrical Slopes ..	1343
Design of a Multilayer Composite-Antenna-Structure by Spiral Type	1348
Impact Behavior of Composite-Surface-Antenna Having Dual Band	1352
From Piezoelectric Actuator to Piezomotor	1357
A Comparison on the Radioelectric Propagation along Grasslands and Scrublands at Wireless Frequency Bands	1362
Design and Development of an Electronic Cowbell Based on ZigBee Technology	1366
RFID from Farm to Fork: Traceability along the Complete Food Chain	1370
Recent Evolution of ITU Method for Prediction of Multipath Fading on Terrestrial Microwave Links ..	1375
Ultra-wideband Spatio-temporal Channel Sounding with Use of an OFDM Signal in an Indoor Environment	1381
Densitometry of Electromagnetic Field Exposure Due to Wi-Fi Frequency	1385
Channel Characterization Techniques for Wireless Automotive Embedded Systems	1391
Performance Comparison of OFDM, MC-CDMA and OFCDM for 4G Wireless Broadband Access and Beyond	1396
Influence of the Design of Resistance Welding Equipment on the Evaluation of Magnetic Field Exposure of Operators	1400
Matrix Converter Commutation Time Reduction	1406
The Use of Prediction to Improve Direct Torque Control	1411
Measurement and Signal Processing for Electric Drive Control System	1416
Sensorless Control of Asynchronous Motor Using Voltage Signal Injection	1421
Comparison of Different Filter Types for Grid Connected Inverter	1426
Soft-switched Converter for Ultracapacitors	1430
Applications of Resonant and Soft Switching Converters	1434
Space Vector Control for Quasi-resonant DC Link Inverter	1438
Optimized Dual Randomized PWM Technique for Full Bridge DC-DC Converter	1442
Skin Effect in Squirrel Cage Rotor Bars and Its Consideration in Simulation of Non-steady-state Operation of Induction Machines	1451
Direct Electromagnetic Torque Control of Induction Motors Powered by High Power PWM Inverters for Two Levels or Three Levels	1456
Broad Antireflection Grating by Apodization of One Dimensional Photonic Crystal	1461
High Frequency Back Scattering from a Real-scale Aircraft Using SBR and PTD-EEC Method	1465

Thin Wires Structure for Decoupling of Multiple-antenna Terminals	1470
Localized EBG Structure with DeCaps for Ultra-wide Suppression of Power Plane Noise	1474
Electromagnetic Field Interaction between Overhead High Voltage Power Transmission Line and Buried Utility Pipeline	1478
Multimode Asymmetrical Optical Power Splitter Utilizing Hollow Structured-waveguide	1483
Localized Optical Modes and Enhancement of Some Optical Phenomena in Spiral Media	1487
Photonic Crystal Based on CdSe Nanoparticles Embedded in a Glass Matrix	1495
Evaluating RF Signal Transmission over Radio-on FSO Links Using Aperture Averaging	1499
Numerical Analysis of Novel Asymmetric SNOM Tips	1505
Electromagnetic Design of Solar Collectors	1512
Channel Estimation in Through-The-Earth Communications with Electrodes	1516
Noise Characterization in Through-The-Earth Communications with Electrodes	1521
Detection of Movement and Impedance Changes behind Surfaces Using Ground Penetrating Radar ..	1526
NLOS UWB Undermining Experimental Characterization & Performance Evaluation Using MB-OFDM	1530
The Effects of Defects on Magneto-inductive Waveguide	1535
Peak to Average Power Ration Reduction in OFDM System Using Constant Envelope for Transmission via PLC Channel	1540
Study of the Impact of Soft Faults on Multiconductor Transmission Lines	1545
Modeling and Diagnostic of Stator Faults in Induction Machines Using Permeance Network Method ..	1550
Interference from the Second Layer in Holographic Radar	1560
A Quasi Linear Sampling Method in Electromagnetic Inverse Scattering	1565
Bistatic Radar Target Classification Using Time-frequency Analysis and Multilayered Perceptron Neural Network	1569
Low Frequency Radar Target Imaging Using Ramp Response Signatures in Arbitrary Directions	1572
A Wigner Ville Distribution Based Method for Detection of Gaussian Contaminated Sinusoidal Signal in Frequency Domain	1576
Effects of Millimeter Wave Exposure on Termite Behavior	1581
Heating and Provocation of Termites Using Millimeter Waves	1586
Electromagnetic Information Transfer of Specific Molecular Signals Mediated through Aqueous Systems: Experimental Findings on Two Human Cellular Models	1590
Vectorial Electro-optic Sensors for Microwave Dosimetric Applications	1593
New Techniques to Reduce the Common-mode Signal in Multi-frequency EIT Applications	1598
Human Exposure to Outdoor PLC System	1602
Analysis of Transmit Magnetic Field Homogeneity for a 7 T Multi-channel MRI Loop Array	1607
Using Rectangular-shape Resonators to Improve the Far-end Crosstalk of the Coupled Microstrip Lines	1612
Electromagnetic Model of In-wall Wiring of Indoor Powerline Communications	1617
Analysis of Transmit Performance Optimization Strategies for Multi Channel MRI Array	1622
Harmonic-suppression Using Adaptive Surface Meshing and Genetic Algorithms	1627
A Reliable Lattice-Boltzmann Solver for Electrodynamics: New Applications in Non-linear Media	1632
Developing Sample Holders for Measuring Shielding Effectiveness of Thin Layers on Compound Semiconductor Substrates	1637
Dissipative Losses Evaluation in Magnetic Power Devices with Litz-wire Type Windings	1642
The Minimum Phase Nature of the Transfer Function of the Impulse Radiating Antenna	1647

The Study on Electromagnetic Force Induced Vibration and Noise from a Normal and an Eccentric Universal Motors	1654
Engineering Students' Conceptual Understanding of Electro- and Magnetostatics	1661
A Physical Model of Electro-magnetism for a Theory of Everything	1665
Space Constants of Auxiliary Waves	1670
Characteristic Equations of Strip-slotted Structures	1674
Self-field Theory a Mathematical Description of Physics	1680
Self-field Theory: Cosmological and Biological Evolution May Be Linked	1684
Self-field Theory and General Physical Uncertainty Relations	1689
General Physical Uncertainty Relations as a Consequence of the Lorentz Transformation	1693
Complete Imitation of the Special Theory of Relativity by the Means of the Classical Physics	1697
FET-based Frequency Multiplier S-MMICs up to 440 GHz	1702
Compact Non-degenerate Dual-mode Filter with Adjustable Transmission Zero	1706
6 × 3 Microstrip Beam Forming Network for Multibeam Triangular Array	1711
Comparative Study of Two Microstrip Beam Forming Networks for Multibeam Triangular Array	1715
Automatic Design and 3D Electromagnetic Simulation of Sub-nH Spiral Inductors	1719
A Novel Dual-mode Dual-band Bandpass Filter with DGS	1723
New Compact Dual-band Filter Using Common Resonator Sections and Double-diplexing Structure	1727
Comparative Study of RF Dual-band-pass Filter	1731
Vectorial Remote Sensing of Guided Electric Field with Pigtailed Electro-optic Microcavities	1734
Incorporation of Optical Fiber-loop and FBG as Displacement and Temperature Sensors for Structure Monitoring	1740
Multi-long-period Gratings for the Optimization of Pump Absorption in Microstructured Optical Fiber Lasers	1744
Two-components Electric-field Sensor for Ultra Wide Band Polarimetric Measurements	1749
A Novel Idea of Quantum Cryptography Coupled with Handover Satellite Constellation for World Cover Communications	1754
Statistical Modelling of the Polarization Mode Dispersion in the Single Mode Optical Fiber Links	1760
Electromagnetic Compatibility of Portable RF Emitters in Uniquos Health Environment: Regulatory Issues	1765
Three Dimensional Safety Distance Analysis around a Cellular Base Station	1770
Application of the Green's Function to Calculating the Impedance of a Uniform Current Density between Two Multilayered Media	1775
Heavy Ions Acceleration of Solar Wind in Electromagnetic and Gravitational Fields	1780
Magneto-optic and Electro-optic Effects in Electromagnetic Fields	1785
Test Method for Evaluating Asphalt-covered Concrete Bridge Decks Using Ground Penetrating Radar	1790
Characterization of the GPR Surface Waves for Civil Engineering Applications	1794
Simulation and Detection Limit of EM Waves in Masonry Structures with Application of an Algorithm for Image Processing	1799
GPR Limits for Thin Layers in Concrete Detection: Numerical and Experimental Evaluation	1804
Insulated Concrete form Void Detection Using Ground Penetrating Radar	1808
Prospective Applications of EM fields in Medicine	1816
Applicators for Research of Biological Effects of EM Field	1822
Microwave Applicators for Industrial Purposes	1825
Closed-form Green's Functions for Stratified Uniaxial Anisotropic Medium	1830

Sidelobe Reduction in Offset Dish Parabolic Antennas Using Metallic Scatters	1835
Computational Electromagnetic Tools for EMC in Aerospace	1840
An Efficient Computational Method Based on Current Measurements for Fields Radiated by a Thin Antenna or a PLC Line	1845
Multi-GPU Accelerated Finite-difference Time-domain Solver in Open Computing Language	1850
Artificial Neural Network Modeling of Synchronous Reluctance Motor	1854
Effect of Ga-doping on the Magnetic and Magnetocaloric Properties of (LaCaSr)(MnGa)O ₃ Compound	1859
The Design of a GPR Test Site for Underground Utilities	1864
A New Algorithm to Estimate the Size of an Underground Utility via Specific Antenna	1868
Combining Multi-frequency GPR Images and New Algorithm to Determine the Location of Non-linear Objects with Civil Engineering Applications	1871
Matching Technique Design for Multi-fed Full Wave Dipole Antenna	1875
Accurate Approximation of Error Probability for Two Types of Adaptive Antenna-based Receivers over Fading Channels	1880
Author Index	1885